X-ray diffraction study of crystal transformation and molecular disorder in poly(tetrafluoroethylene)

Takashi Yamamoto and Tetsuhiko Hara
Department of Physics, Faculty of Science, Yamaguchi University, Yamaguchi, Japan
(*Received* 6 *May* 1981; *revised* 20 *July* 1981)

The intermolecular and intramolecular disorders, and the crystalline phase transition in poly(tetrafluoroethylene) are examined by X-ray diffraction between 20° and 250°C. A presence of the crystalline phase transition around $T_t = 150$°C is confirmed by the rapid decrease in the intensity of the Bragg reflection 1015. This phase transition is ascribed to the abrupt increase of the intermolecular translational disorder along the chain. From the quantitative analysis of the profile of the 0015 reflection, it is found that the increase in the translational disorder described above is accompanied by the excitation of the intramolecular disorder in conformation. The intramolecular disorder in conformation below T_t is found to be due mainly to the thermal excitation of *trans* conformation in the usual 15–7 helix. Further increase in disorder in conformation is found above T_t, which is due to the excitation of *gauche* conformation. The fraction of *trans* conformation increases up to 40% with the increase of temperature, in good agreement with the theoretical calculation. The fraction of *gauche* conformation above T_t is also estimated to give, for example, 7.5×10^{-3} at $T = 214$°C.

Keywords Diffraction; X-ray diffraction; crystal transformation; poly(tetrafluoroethylene); intermolecular disorder; intramolecular disorder

INTRODUCTION

Disorders in macromolecular crystals can be put into two categories from a geometrical point of view: intermolecular and intramolecular disorders. These are further classified into static and dynamic disorders according to the origins of the disorders. Disorder introduced through plastic deformation of the crystals and that caused by the presence of chemical defects in the chain molecules such as branches, are the examples of the intermolecular and intramolecular disorders respectively, both of static nature. The disorders usually discussed are these static disorders[1,2]. Since these disorders have different origins, they have been treated as separate problems. The disorders we shall discuss are dynamic disorders thermally excited at high temperatures.

Thermally excited disorders, especially intramolecular disorder, are considered to play an important role in the translational motion of the molecules along the chain axis[3]. They are also closely related to the phase transition phenomena in polymer crystals[4-6].

Though detailed energetical discussions were done for the possibility of the translational diffusion of the molecules along the chain axis in the crystals[7,8], there is little direct experimental evidence for the translational motion of the chain.

Recently, crystalline phase transitions of order-disorder type were found in some polymeric crystals, where uniformly ordered helical molecules transform to the disordered ones[4-6]. These disordered molecules may be considered as coiled molecules confined in crystalline potential fields generated by the neighbouring chains. Poly(tetrafluoroethylene) (PTFE) is one of these few polymers which have such highly disordered phases, as will be described later in this paper.

The crystal of PTFE is known to have two crystalline transitions at 19°C and 30°C under atmospheric pressure[9]. Below 19°C the molecules are in an ordered 13–6 helical conformation with little intermolecular disorders, if any. Above 19°C the molecules transform to 15–7 helix with intermolecular disorder. As fully discussed by Clark and Muus[10], the disorder between 19°C and 30°C is that of rotational freedom of the chain molecule around the chain axis.

The aim of this paper is firstly to show the presence of intermolecular translational disorder along the chain axis above room temperature, which exhibits a phase transitional behaviour around 150°C. Secondly to clarify the presence of intramolecular disorder and to evaluate the fraction of the disordered portion in the chain by assuming a molecular model of the disordered conformation. It is also shown that the intramolecular disorder is enhanced by the increase of intermolecular disorder.

EXPERIMENTAL

The fibre of PTFE (E. I. du Pont de Nemours and Company) was used as a sample. It was annealed at 260°C, kept in constant length, for a day in a silicon oil bath. During the X-ray experiment the fibre, which was held by metal sample holder, was heated up to 250°C by blowing hot air generated by a resistance furnace. The temperature of the sample was measured by copper-constantan thermocouple. It was controlled within

0032-3861/82/040521-08$03.00

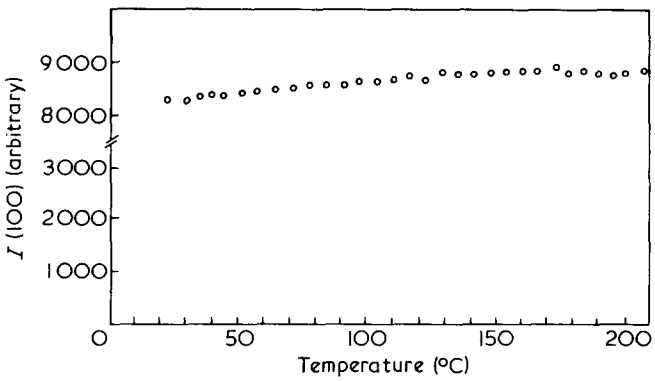

Figure 1 The temperature dependence of the integrated intensity of 100 reflection

± 0.1°C by regulating the power of the furnace with a PID controller.

Point focused incident beam of X-ray (Cu Kα) was transmitted symmetrically through the sample, whose thickness was ~0.5 mm. Measurements of the intensities of the diffraction were made using a scintillation counter and a goniometer with step scan facility controlled by a microcomputer. Scan increments were 0.02° or 0.05° as appropriate. Monochromatization was made using Ni filter and pulse height analyser.

RESULTS AND DISCUSSION

Intermolecular translational disorder

Before discussing the translational disorder along the chain in a crystal, we must estimate a degree of the transverse disorder, that is, a disorder in the average position of the chain in the plane perpendicular to the chain axis. *Figure 1* shows a change of the integrated intensity of the equatorial Bragg reflection 100 with temperature. It is seen that the integrated intensity of the reflection shows little change with temperature.

Following the calculation done by Clark and Muus[11], a decrease in the intensities of the Bragg reflections on the 1-th layer line due to the rigid rotation or translation of the molecules can be written as:

$$I = I_0 \exp(-n^2\overline{\Delta\varphi^2}) \exp(-4\pi^2 \underset{\sim}{l}^2 \cdot \overline{\Delta Z^2}/c^2) \qquad (1)$$

where c is a fibre period, n is the least integer which satisfies the equation $\tilde{l} = 15m + 7n$, and $\overline{\Delta\varphi^2}$ and $\overline{\Delta Z^2}$ are the mean square amplitudes of the rotational and the translational motion of the molecules respectively. In this expression, the correlation between $\Delta\varphi$ and ΔZ is neglected. The least value of n for the equator, $\tilde{l} = 0$, is zero, and therefore the intensities of the Bragg reflections on the equator should not change by the rotation or the translation of the molecules. The experimental result shown in *Figure 1* supports this conclusion, and at the same time it also shows that the degree of the transverse disorder in the lateral packing of the molecules is kept constant within the temperature range of our present experiment. In other words, the temperature factor $D_\perp$ for the direction perpendicular to the chain axis is considered to be independent of temperature.

The intensities of the Bragg reflections on the 15-th layer line can also be written by the zeroth order Bessel function J_0[11]. They must not therefore decrease by the mere rotation of the molecules around their axes. X-ray photographs in *Figure 2* show the change with temperature of the 0015 and 1015 reflections of PTFE. As the temperature increases, the intensity of the reflection 1015 decreases rapidly accompanied by the increase of the diffuse streak scattering on the 15-th layer line. In *Figure 3*, the profiles of 1015 reflection at four different temperatures are given. They were obtained by step scanning parallel to the meridional direction. A rapid decrease in intensity is evidently seen with the increase of temperature. Since the temperature factor $D_\perp$ for the direction perpendicular to the chain axis is independent of temperature, the decrease in the intensity of 1015 reflection is considered to be due to the intermolecular translational disorder: the latter exponential term in equation (1).

The background scattering on the low angle side of the peak in *Figure 3* is due to the diffuse streak on the 15-th layer line. A separation of the Bragg component from the observed profile shown in *Figure 3* was done by assuming a profile of the diffuse scattering component from the profile obtained at high temperature where Bragg component actually vanishes. The intensity of the Bragg reflection 1015 obtained in this way is plotted against temperature in *Figure 4*.

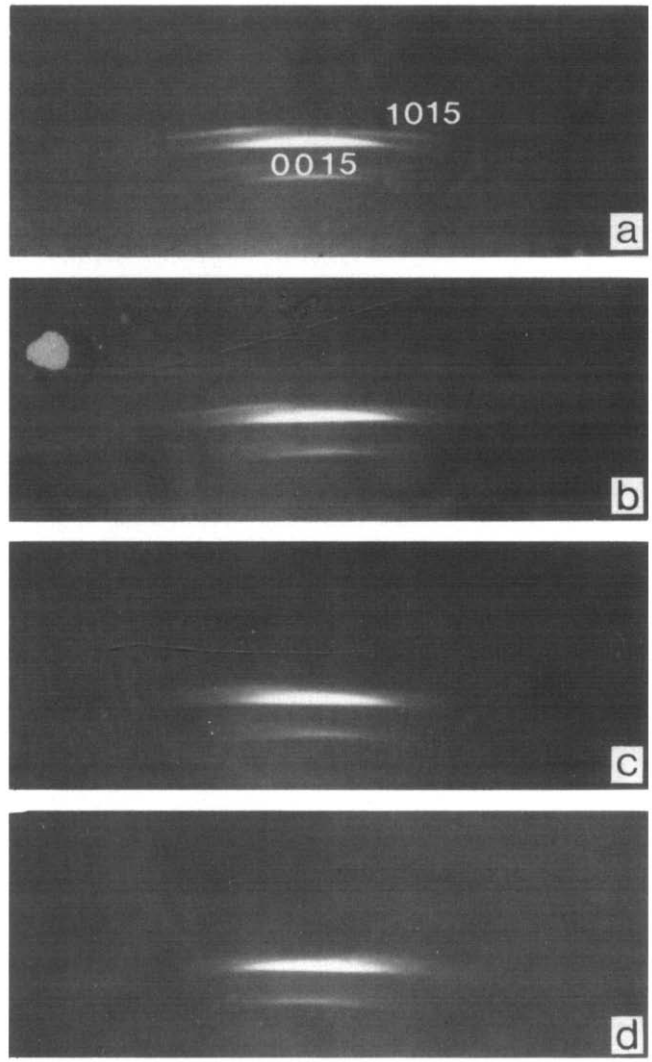

Figure 2 X-ray diffraction photographs of 0015 and 1015 reflections at (a) 20°C, (b) 84°C, (c) 120°C, (d) 150°C

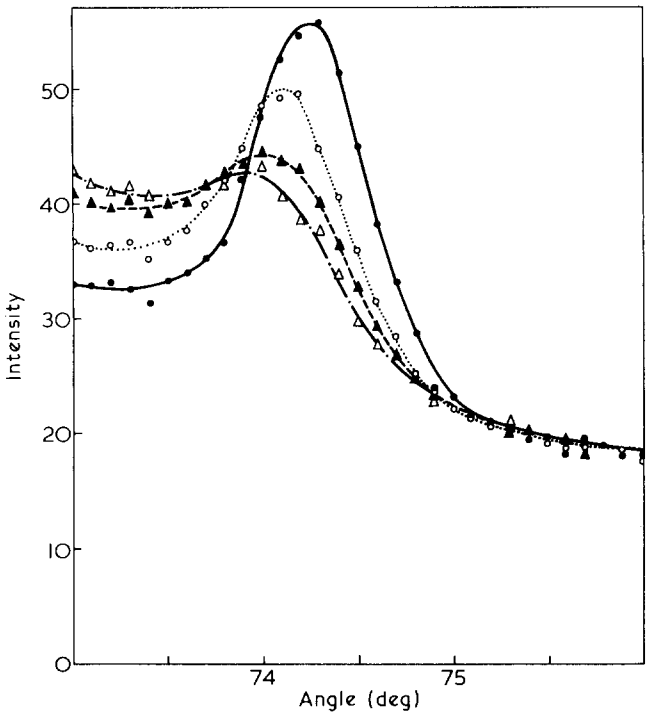

Figure 3 X-ray diffraction patterns of 1015 reflection at (●) 20°C, (○) 83°C, (▲) 136°C, and (△) 156°C, obtained by step scanning parallel to the meridional direction

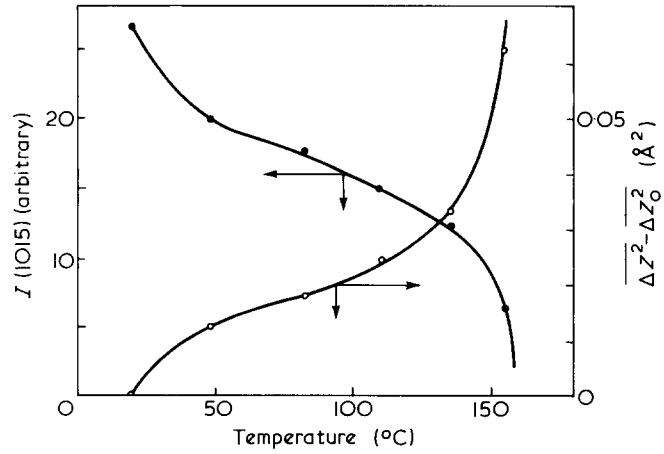

Figure 4 The changes of the intensity of 1015 reflection (●) and the degree of the translational disorder along the chain, $\overline{\Delta Z^2}-\overline{\Delta Z_0^2}$, (○) as a function of temperature

When a translational or screw motion of the chain molecules is considered, the decrease in the intensity of 1015 Bragg reflection is written, from equation (1), as:

$$I_B/I_{B0}=\exp\{-4\pi^2 l^2(\overline{\Delta Z^2}-\overline{\Delta Z_0^2})/c^2\} \qquad (2)$$

where $l=15$, I_B and $\overline{\Delta Z^2}$ are the intensity of the reflection 1015 and the mean square translational displacement of the chain along the chain axis respectively at any temperature, and I_{B0} and $\overline{\Delta Z_0^2}$ are those at room temperature. In *Figure 4* the change of $\overline{\Delta Z^2}-\overline{\Delta Z_0^2}$ with temperature calculated through equation (2) is shown. As the temperature approaches 150°C, the intermolecular translational disorder, $\overline{\Delta Z^2}-\overline{\Delta Z_0^2}$, becomes infinitely large. Thus presence of the phase transition, T_t, around 150°C is evident. It can be said that the phase transition at T_t is associated with the translational freedom of the chain, while those at 19°C and 30°C are associated with the rotational freedom.

It is expected that the presence of the phase transition at T_t may result in anomalies in the packing of the molecules. *Figure 5* shows a change of the lattice spacing $d(100)$ with temperature. As expected, we can see an abrupt change in slope of $d(100)$ vs. T curve near T_t. The linear expansion coefficients in lateral direction under and above T_t are estimated to be 7.5×10^{-5} deg^{-1} and 9.3×10^{-5} deg^{-1} respectively. An abrupt release of the close packing of the molecules due to both the rapid increase of the translational disorder and the increase of conformational disorder, which will be described later in this paper, is considered to result in the above mentioned knick near T_t.

In many mechanical relaxation experiments on PTFE, a relaxational absorption was observed near T_t. Though some ambiguity still remains in the assignment of the mechanism of the absorption, this absorption has been considered as a glass transition I, the glass transition in the paracrystalline region, from the dependence of the absorption intensity on crystallinity[12,13]. Our experimental results, however, indicate that the transition at T_t occurs in the usual crystalline regions. This apparent contradiction cannot be explained adequately at present, but it seems to suggest some coupling effect of the amorphous and the crystalline regions.

Intramolecular disorder

As described in the previous section, the intermolecular disorder increases rapidly as the temperature reaches T_t. This suggests the increase of intramolecular disorder in the chain near T_t and below. Further increase of disorder in the conformation is expected above T_t, since the chain molecules in the crystal above T_t are fairly free from the constraint by the crystalline field, that is, a constraint to set molecules into crystallographic register.

Since potential barriers to the translation and the rotation of the molecules are more or less smeared out, the molecules in the crystals of PTFE at high temperatures may be considered as being confined in a cylindrical potential generated by the neighbouring chains. The problem of the excitation of the conformational disorder in PTFE crystals can, therefore, be imagined as a sort of helix-coil transition for the chain molecules confined in such cylindrical potentials.

Figure 6 shows a change in the profile of 0015 reflection with temperature obtained by step scanning along the

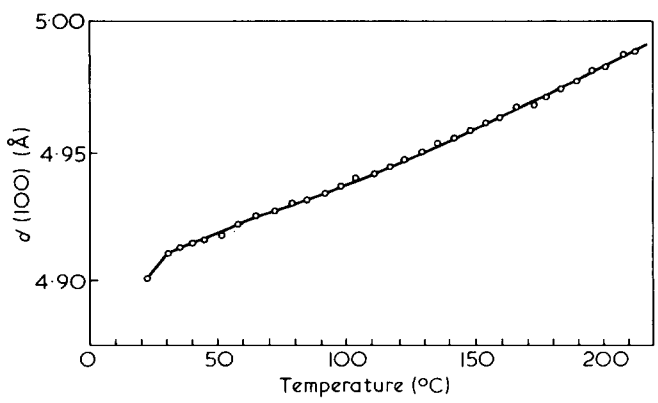

Figure 5 Lattice spacing $d(100)$ as a function of temperature

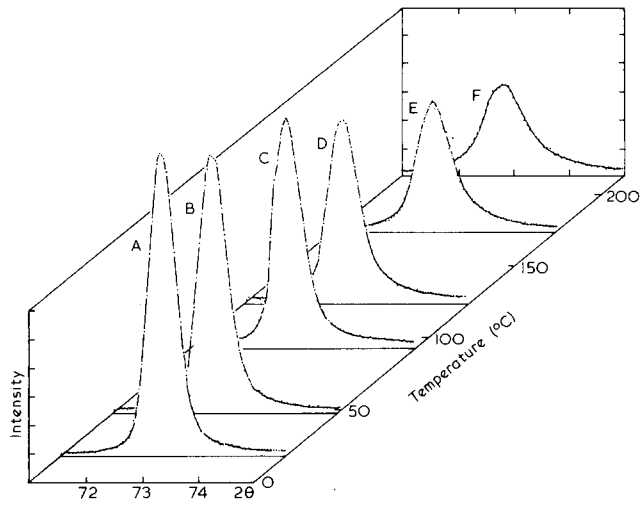

Figure 6 X-ray diffraction patterns of 0015 reflection at (a) 19°C, (b) 49°C, (c) 94°C, (d) 135°C, (e) 175°C, and (f) 214°C, obtained by step scanning along the meridian

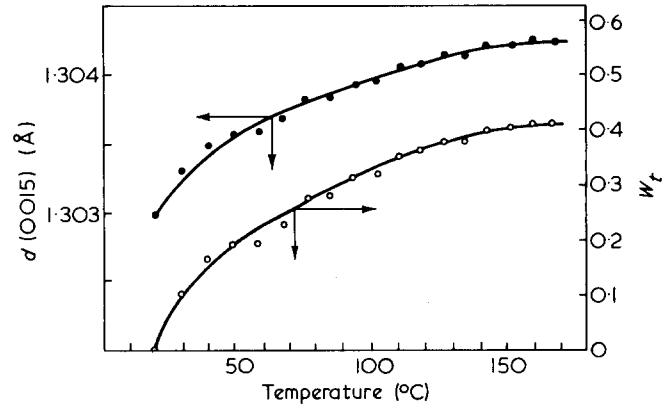

Figure 7 The temperature dependences of the lattice spacing d(0015) (●) and the fraction of t subunit, w_t, in the chain (○)

meridian. Remarkable changes can be seen in peak intensity, integrated intensity, apparent width, and peak position.

Firstly, we pay our attention to the temperature dependence of the spacing d(0015) (*Figure 7*). The value of d(0015) increases monotonously with the increase of temperature, and levels off at approximately T_t. Since the profile of the reflection becomes a very broad one above T_t, the precise determination of d(0015) could not be done above T_t due to experimental error.

As described before, there seems to be a conformational disorder in the chain above room temperature. The change of d(0015) with temperature can be well understood through the increase of conformational disorder as follows.

The equilibrium conformation of PTFE molecules at room temperature is 15–7 helix, and the internal rotation angles are deviated $\sim \pm 14°$ from those of all *trans* conformation corresponding to the right or the left handed helix. We denote CF_2 subunit in the usual 15–7 helical conformation and that in all *trans* conformation by $t^{\pm}$ and t respectively. Since the potential barrier to the internal rotation between $t^{\pm}$ states and t state is small, the conformational disorder in the molecules of 15–7 helix most easily excited at high temperatures is considered to be due to the excitation of t subunits in the chain. In the following discussion, we assume that $t^{\pm}$ and t subunits are distributed at random in the chain. The correlation in the succession of these three types of subunit is not discussed here.

Following a similar argument to our previous work[6], the intensity of the diffraction on the meridian can be written by the scattering intensity $\langle |F|^2 \rangle$ from a single disordered chain. Taking CF_2 group as a scattering unit in the chain, the intensity of the scattering from the chain can be written:

$$\langle |F|^2 \rangle = N_c |\bar{f}|^2 \cdot D^2 \cdot Z(S_z) \tag{3}$$

$$Z(S_z) = Re\left(\frac{1+G}{1-G}\right) \tag{4}$$

$$G(S_z) = (1-w_t)\exp(2\pi i C_0 S_z) + w_t \exp(2\pi i C_t S_z) \tag{5}$$

where z axis is taken parallel to the fibre axis, S_z is a Z component of the scattering vector $\underline{S}$, N_c is the number of subunits in the chain, $\bar{f}$ is an averaged structure factor of the subunit, D is a temperature factor, C_0 and C_t are the projected length of $t^{\pm}$ and t subunits respectively on the Z axis, and w_t is a fraction of t subunit in the chain (*Figure 8*). Equation (5) can be obtained by the Fourier transformation of the following pair distribution function $H_1(z)$, instead of usual Gaussian distribution, in the one dimensional paracrystal theory of diffraction.

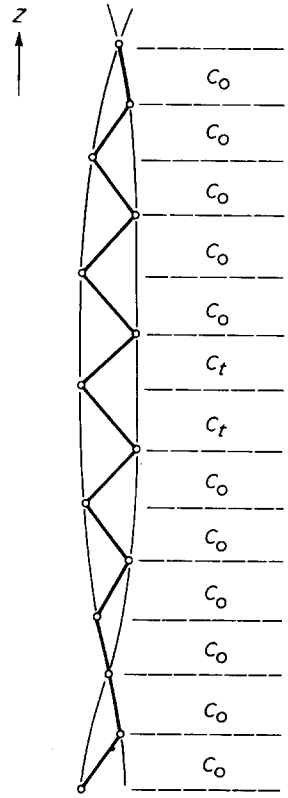

Figure 8 The schematic picture of the disordered conformation of PTFE molecules below T_t. The letter C_0 and C_t stand for the projected length of $t^{\pm}$ and t subunits respectively on Z-axis, and taken as C_0 = 1.303 Å and C_t = 1.306 Å. These values for C_0 and C_t are calculated from the values of C–C bond length r = 1.54 Å, C–C–C bond angle ϕ = 116°, and the internal rotation angle τ_0 = 14° and τ_t = 0°

$$H_1(z)=(1-w_t)\cdot\delta(z-C_0)+w_t\cdot\delta(z-C_t) \quad (6)$$

where δ represents Dirac delta function. Through equation (3), the relation between the averaged spacing $\bar{C}$, which is determined from the peak position of 0015 reflection, and the population of t subunits w_t can be calculated, and the following simple relation is fulfilled:

$$\bar{C}=(1-w_t)C_0+w_tC_t \quad (7)$$

This type of equation, which is usually called Vegard's rule, has been frequently used in metallurgy for the solid solution of two component metals. Now it is found that the same equation can be used to estimate the fraction of t subunit in the succession of $t^{\pm}$ and t subunits in the molecules. It should be emphasized, however, that this equation holds only for the case where the difference C_0-C_t is sufficiently small.

From *Figure 7* (the upper curve) and equation (7), the fraction of t subunit in the chain, w_t, is estimated to give the result shown also in *Figure 7*. The population of t subunits increases monotonously with the increase of temperature until it reaches the value of $\sim 40\%$ around T_t. The temperature T_t was defined as a transition point to a disordered state in the intermolecular translational freedom. *Figure 7*, therefore, shows a definite correlation between intermolecular and intramolecular disorders. The increase in the conformational disorder near T_t may cause the decrease of the interchain potential barrier to the translational motion of the molecules along the chain, and may lead to the disordered state in the translational freedom along the chain.

It is widely accepted that the intramolecular energy for the excitation of t subunit in a chain is small in comparison with the thermal energy RT at room temperature[14]. Simple thermodynamical argument shows that the fraction of t subunit in the free chain, free from crystalline constraint, is $\sim 30\%$ at room temperature and above. (Better estimate by Corradini and Guerra gives a similar result of ~ 24–32%[15].) *Figure 7* shows that the fraction of t subunit in the chain comes close to the above theoretical value for the free chain near T_t.

In an ordered state of the crystal of PTFE below room temperature, the requirement of three dimensional ordering in packing the molecules suppresses the increase of conformational disorder. The increase of translational disorder at high temperatures replaces the above requirement by more generous one: parallel packing of the molecules. Since the introduction of t subunits into the chain does not seriously violate the requirement of the parallel packing of the molecules[15], the population of the t subunits can come close to the corresponding value for the free molecules of $\sim 30\%$ in the translationally disordered state near T_t.

In *Figure 9* the peak intensity and the apparent half width of 0015 reflection are plotted as a function of temperature. A remarkable increase of the width is seen above T_t accompanied by a decrease of the peak intensity. An interpretation of the width of the reflection is somewhat complicated. As described previously, the intermolecular translational disorder becomes infinitely large near T_t. From equation (1) the Bragg reflection 0015 also should decrease its intensity rapidly near T_t and disappear above T_t. The observed reflection 0015 above T_t, though it seems a Bragg reflection, should therefore be regarded as a diffuse streak scattering concentrated on the meridian. This conclusion is also verified by the following quantitative consideration of the profile.

The profile of the 0015 reflection can be written as a sum of the contributions from Bragg reflection 0015 and diffuse streak on the 15-th layer line. At a relatively low temperature, where there is little intermolecular translational disorder, the contribution from the diffuse streak can be neglected. By the rapid decrease and increase of the Bragg reflection 0015 and the diffuse streak respectively near T_t, both due to the increase of the intermolecular translational disorder, the contribution from the diffuse streak scattering begins to dominate the profile of the reflection. The profiles of both contributions, I_B^{obs} for Bragg contribution and I_D^{obs} for diffuse contribution, obtained by scanning along the meridian can be written as follows (Appendix):

$$I_B^{obs}=I_{instr}\widehat{I_{size}}\widehat{I_{intra}} \quad (8)$$

$$I_D^{obs}=\widehat{I_{B0}^{obs}}I_{D0} \quad (9)$$

where $\widehat{\ }$ denote convolution, I_{instr} is an instrumental profile and it does not depend on temperature, I_{size} and I_{intra} stand for the line broadening effects due to the finite crystal size and the intramolecular disorder of the second kind respectively, I_{D0} is a complicated function given in equation (A-5) in the Appendix. Since the melting point of PTFE crystal is higher than the temperature range of our present experiment, the change of the lamella thickness can be neglected. The effect of the lamella thickness on the profile of 0015 reflection through shape factor, I_{size}, is therefore independent of temperature. Furthermore, the effect of the intramolecular disorder, I_{intra}, is negligible at room temperature, where PTFE molecules are in conformationally ordered state. The profile of the Bragg reflection at room temperature, I_{B0}^{obs}, is therefore taken as an effective instrumental profile in equation (9).

The disordered chain is considered to consist of only $t^{\pm}$ and t subunits. Since the difference of C_0 and C_t is small enough to be neglected in the present discussion of the profile, the increase of the width with temperature of the Bragg reflection 0015, I_B^{obs}, is negligible. The change in the width of the reflection observed below T_t should, therefore, be ascribed to the increase of the diffuse streak scattering I_D^{obs}. The profile of the reflection at T_t, where the Bragg reflection 0015 disappears, is given by equation (9).

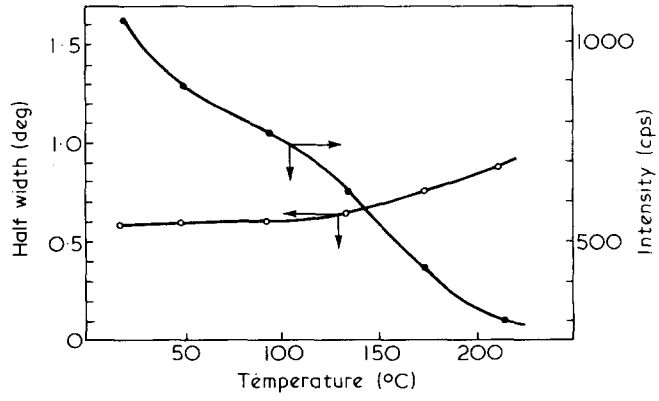

Figure 9 The temperature dependences of the peak intensity (●) and the half width (○) of 0015 reflection

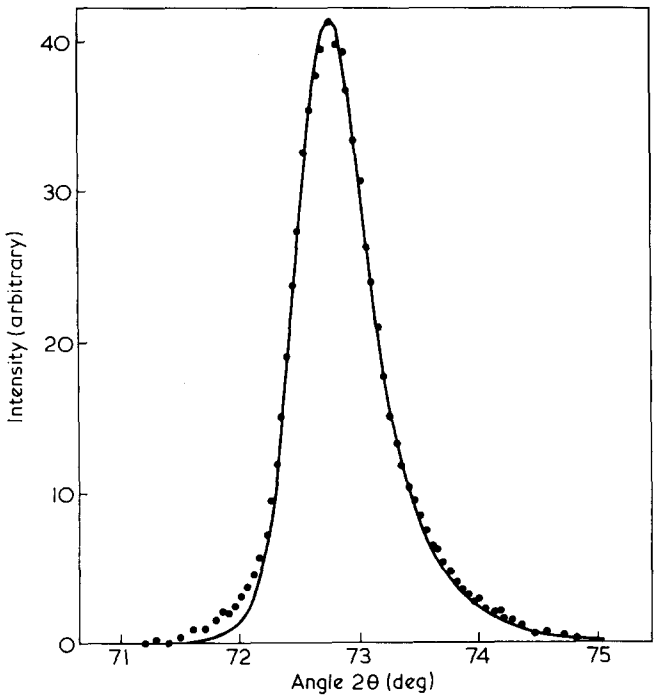

Figure 10 The comparison of the calculated profile of equation (9) (———), where r = 1.64 Å for fluorin helix and $\beta = 8.7 \times 10^{-2}$ radian, and the observed profile at 175°C (●)

Rigorous evaluation of equation (9) was done by Fourier transformation methods. The procedure is similar to Stokes method in the slit correction[16]. The calculated profile of equation (9) and the observed one near T_t are given in *Figure 10*. These two profiles show good agreement. Thus it is reasonable to think that the apparent increase in width of the reflection below T_t is mainly due to the increase in the intensity of diffuse streak scattering accompanied by the decrease in that of Bragg reflection.

Further increase in the width of the reflection above T_t is, on the contrary, considered to be due to the increase of conformational disorder of the second kind. We found that the population of t subunits in the chain approaches near T_t to the maximum value expected from thermodynamics. The possible additional disorder in the conformation above T_t may be, therefore, due to the excitation of *gauche* subunits; $g^{\pm}$. For simplicity we assume that the ratio of the population of t and $t^{\pm}$ subunits above T_t is the same as that at T_t, and define the averaged subunit $\bar{t}$ as having an averaged structure factor and the averaged period: $C_{\bar{t}} = 0.6C_0 + 0.4C_t$. The disordered conformation above T_t is now simplified as a sequence of $\bar{t}$ and $g^{\pm}$ subunits.

By a similar treatment as equations (3)–(5), $\langle |F|^2 \rangle$ can be written:

$$\langle |F|^2 \rangle = N_c |\bar{f}|^2 \cdot D^2 \cdot Z(S_z) \tag{10}$$

$$Z(S_z) = Re\left(\frac{1+G}{1-G}\right) \tag{11}$$

$$G(S_z) = (1 - W_g)\exp(2\pi i C_{\bar{t}} S_z) + W_g \exp(2\pi i C_g S_z) \tag{12}$$

where W_g is a fraction of $g^{\pm}$ subunit, and C_g is a projected period of $g^{\pm}$ subunit on the chain axis and is taken at $C_g = 0.96$ Å by assuming that a local disordered conformation is a sequence of *gauche* subunits with internal rotation angle $\tau_g = \pm 120°$.

The observed profile above T_t is then given by the convolution of the theoretical profile given in equation (10) and the effective instrumental profile for the diffuse streak scattering I_{D0}^{obs} (Appendix).

$$I_D^{obs} = \widehat{I_{D0}^{obs} \langle |F|^2 \rangle} \tag{13}$$

The calculation of equation (13) was done through Fourier method as before. *Figure 11* shows a change of the apparent half width with the fraction of $g^{\pm}$ subunit, w_g, calculated through equation (13). A comparison of the calculated profile of equation (13) for $w_g = 7.5 \times 10^{-3}$ and the observed one at 214°C, as an example, is shown in *Figure 12*. In *Figure 12*, a remarkably good agreement is attained. Especially, the asymmetry of the profile due to the presence of a tail at higher angle side of the peak is well reproduced.

The fraction of $g^{\pm}$ subunit, w_g, estimated in this way is plotted against temperature in *Figure 13*. Though the value of 0.75% for the fraction of *gauche* subunit w_g at 214°C seems to be very small, we have no other information to compare with our result at present. We have to conclude, therefore, that this is a most plausible value for w_g as far as our present experiment is concerned.

CONCLUSION

From X-ray diffraction study of PTFE, the crystal transformation around $T_t = 150$°C was found. It is attributed to the rapid increase in the intermolecular translational disorder of the chain molecules. This increase in the translational disorder was found to be accompanied by the increase in the intramolecular disorder. The intramolecular disorder below T_t is mainly due to the excitation of *trans* conformation in the usual 15/7 helical conformation of the molecules, and that above T_t is due to the excitation of *gauche* conformation. Thus the crystal

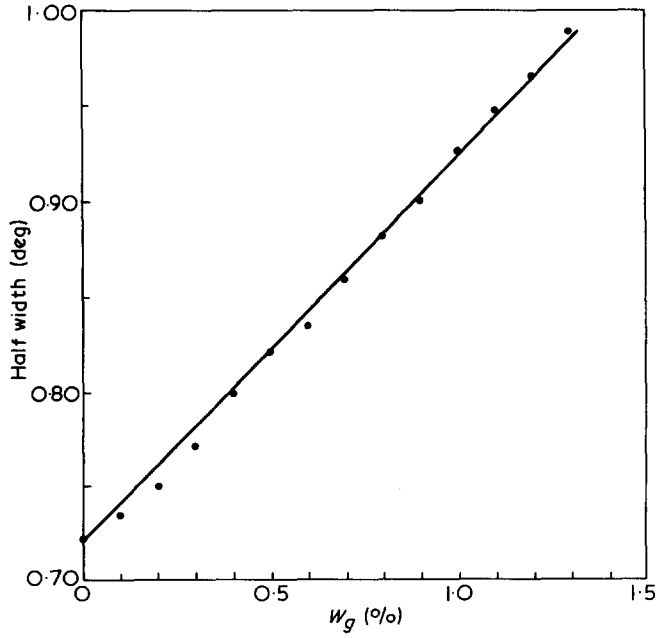

Figure 11 The calculated width of 0015 reflection through equation (13) as a function of the fraction of *gauche* subunit w_g

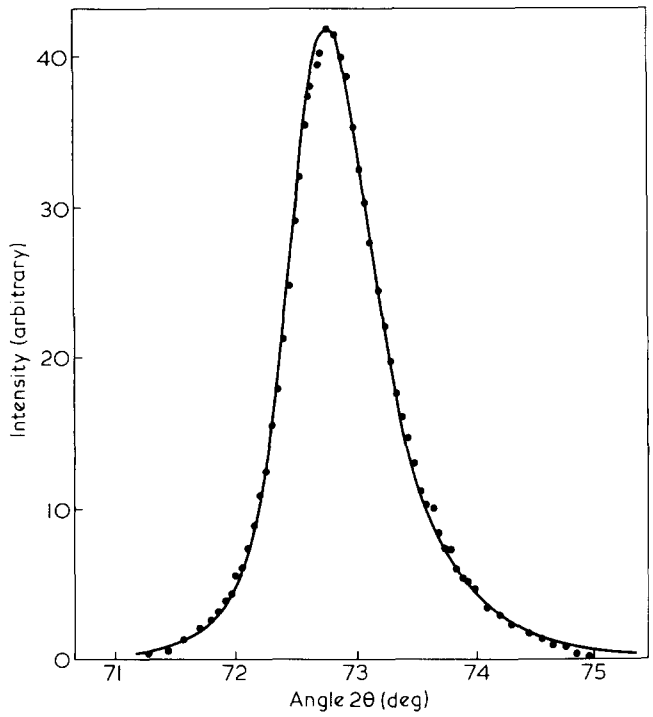

Figure 12 The comparison of the calculated profile of equation (13) for w_g = 0.75% (———), and the observed one at 214°C (●)

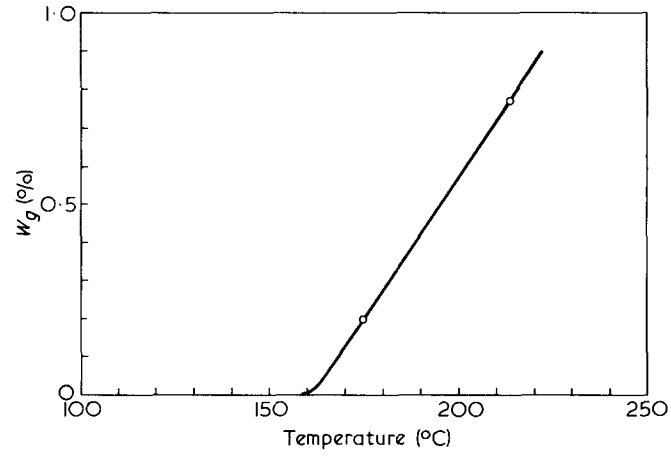

Figure 13 The temperature dependence of the fraction of $g^{\pm}$ sub-unit, w_g, in the chain

transformation at T_t and the molecular disorders associated with this transformation were clarified. The understanding of these facts will supply the basis for further analysis of the crystalline disorders in PTFE.

ACKNOWLEDGEMENT

This work was supported by a Grant-in-Aid of Scientific Research from Ministry of Education.

REFERENCES

1 Buchanan, D. R. and Miller, R. L. *J. Appl. Phys.* 1966, **37**, 4003
2 Wecker, S. M., Cohen, J. B. and Devidson, T. *J. Appl. Phys.* 1974, **45**, 4453
3 Reneker, D. H. *J. Polym. Sci.* 1962, **59**, S39
4 Weeks, J. J., Sanchez, I. C., Eby, R. K. Poser, C. I. *Polymer* 1980, **21**, 325
5 Matsushige, K., Enoshita, R., Ide, T., Yamauchi, N., Taki, S. and Takemura, T. *Jpn. J. Appl. Phys.* 1977, **16**, 681
6 Yamamoto, T. *J. Macromol. Sci.-Phys.* 1979, **16**, 487
7 MacMahon, P. E., McCullough, R. L. and Schlegel, A. A. *J. Appl. Phys.* 1967, **38**, 4123
8 Reneker, D. H., Fanconi, B. M. and Mazur, J. *J. Appl. Phys.* 1977, **48**, 4032
9 Bunn, C. W. and Howells, E. R. *Nature* 1954, **174**, 549
10 Clark, E. S. and Muus, L. T. *Z. Kristallogr.* 1962, **117**, 119
11 Clark, E. S. and Muus, L. T. *ibid* 1962, **117**, 108
12 McCrum, N. G. *J. Polym. Sci.* 1959, **34**, 355
13 Ohzawa, Y. and Wada, Y. *Jpn. J. Appl. Phys.* 1964, **3**, 436
14 Bates, T. W. *Trans. Faraday Soc.* 1967, **63**, 1825
15 Corradini, P. and Guerra, G. *Macromolecules* 1977, **10**, 1410
16 Stokes, A. R. *Proc. Phys. Soc. (London)* 1948, **61**, 382
17 Guinier, A. 'X-ray Diffraction in Crystals', W. H. Freeman, San Francisco, 1963

APPENDIX

The profile of a Bragg reflection can be written as a convolution of three factors[17]:

$$I_B^{obs} = I_{instr} \widehat{I_{size}} I_{intra} \qquad \text{(A-1)}$$

where I_{instr}, I_{size} and I_{intra} represent the instrumental profile, the line broadening effect due to finite size of the crystals, and that due to intramolecular disorder of the second kind. The analysis of the diffuse streak scattering, on the contrary, requires some additional geometrical considerations. In this Appendix, we calculate the profile along the meridian of the diffuse streak scattering on the 15-th layer line.

The difference between Bragg reflection and diffuse scattering is that the latter has an appreciable width in the intensity distribution along the layer line. This causes the increase in the apparent width along the meridian, if the distribution in the orientation of the fibre axis cannot be ignored.

The contribution of the crystallites, whose fibre axes depart from the averaged fibre axis ζ by the angle φ, to the intensity of the diffraction on the meridian is expressed by the following (*Figure 14*):

$$I_{D0}(\zeta)d\zeta = J_0^2(2\pi r D_z^0 \tan\varphi) \cdot P(\varphi)d\varphi \qquad \text{(A-2)}$$

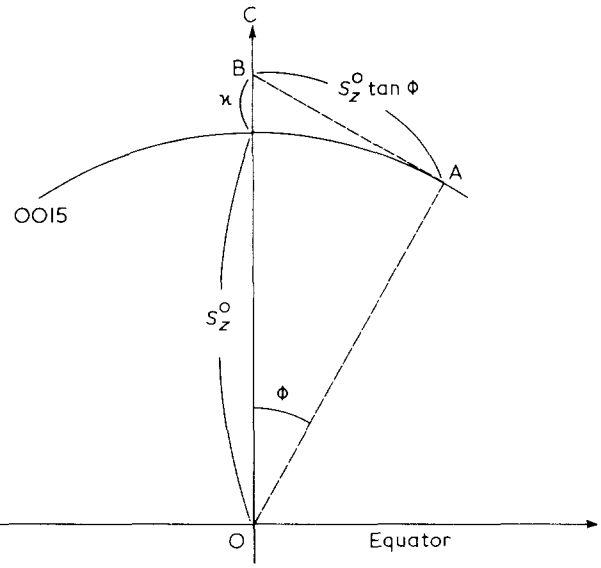

Figure 14 Schematic picture of 0015 reflection to calculate the intensity of the diffraction on the meridian. Crystallites (A) whose fibre axes make an angle of ϕ to the averaged fibre axis C contribute to the intensity at point (B) on the meridian

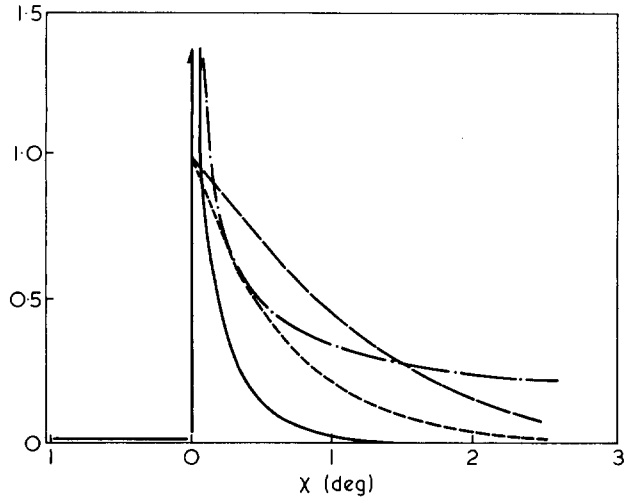

Figure 15 Calculated profile of equation (A2–5) for r = 1.64 Å (fluorin helix), S_z^0 = 0.769 Å^{-1}, and β = 8.7 x 10^{-2} radian. (——) $J_0^2(2\pi r\sqrt{2S_z\zeta})\, e^{-\zeta/S_z\beta^2}\ 1/3\sqrt{\chi}$; (– – – –) $J_0^2(2\pi r\sqrt{2S_z\zeta})$; (· · · · · ·) $e^{-\zeta/S_z\beta^2}$; (– – – · – · – ·) $1/3\sqrt{\chi}$

$$\zeta = S_z^0\left(\frac{1}{\cos\varphi} - 1\right) \tag{A-3}$$

where $P(\varphi)$ represents the distribution of orientation, r is a radius of helix, and $I_{D0}\,d\zeta$ is the intensity of the diffraction on the meridian ζ apart from the reciprocal lattice point 0015. Since φ and ζ are small, equation (A-3) is approximated by:

$$\zeta = \frac{1}{2}S_z^0 \cdot \varphi^2 \tag{A-4}$$

By putting equation (A-4) into (A-2), $I_{D0}\,d\zeta$ can be written:

$$I_{D0}(\zeta)d\zeta = J_0^2(2\pi r\sqrt{2S_z^0\zeta})\frac{1}{\sqrt{2\pi}\beta}\exp\left(-\frac{\zeta}{S_z^0\beta^2}\right)\frac{1}{\sqrt{2S_z^0}}\frac{1}{\sqrt{\zeta}}d\zeta \qquad (\text{for } \zeta \geqslant 0)$$

$$I_{D0}(\zeta)d\zeta = 0 \qquad (\text{for } \zeta < 0) \tag{A-5}$$

where the distribution function P is assumed to be Gaussian:

$$P(\varphi) = \frac{1}{\sqrt{2\pi}\beta}\exp\left(-\frac{\varphi^2}{2\beta^2}\right) \tag{A-6}$$

In *Figure 15*, the calculated profile of equation (A-5) is shown, where the abscissa is written in an angle of deviation χ from the scattering angle $2\theta_0$ of 0015 reflection:

$$\zeta = \chi \cdot \cos\theta_0/\lambda \tag{A-7}$$

In *Figure 15*, the contribution of each term that constitutes the right side of equation (A-5) is also shown.

The observed profile of the diffuse streak scattering is given by the convolution of the calculated profile given in equation (A-5) and the instrumental profile I_{B0}^{obs} as follows:

$$I_{D0}^{obs} = \widehat{I_{D0}\ I_{B0}^{obs}} \tag{A-8}$$

In considering the line broadening above T_t of the diffuse streak scattering due to the increase of conformational disorder, the function I_{D0}^{obs} given above can be regarded as an instrumental profile:

$$I_D^{obs} = \widehat{I_{D0}^{obs}\ \langle|F|^2\rangle} \tag{A-9}$$